Tetrahedron Letters 52 (2011) 4848–4853

Contents lists available at ScienceDirect

Tetrahedron Letters

journal homepage: www.elsevier.com/locate/tetlet

BODIPY-bridged push–pull chromophores: optical and electrochemical properties

Songlin Niu [a], Gilles Ulrich [a,*], Pascal Retailleau [b], Raymond Ziessel [a,*]

[a] Laboratoire de Chimie Organique et Spectroscopies Avancées (LCOSA), UMR7515, ECPM, 25 rue Becquerel, 67087 Strasbourg, Cedex 02, France
[b] Laboratoire de Cristallochimie, ICSN-CNRS, Bat 27-1 Avenue de la Terrasse, 91198 Gif-sur-Yvette, Cedex, France

ARTICLE INFO

Article history:
Received 30 June 2011
Accepted 6 July 2011
Available online 22 July 2011

Keywords:
BODIPY
Push–pull
Cycloaddition
Tetracyano
Fluorescence
Electrochemistry

ABSTRACT

A series of BODIPY bridged push–pull chromophores were prepared by a sequence of reactions involving: i) cross-coupling reactions promoted by palladium complexes; ii) Knoevenagel condensation leading to dicyano derivatives; iii) [2+2] cycloaddition. The last reaction is regioselective, providing mono-derivatives with anisole substituents. With dimethylaminophenyl donor groups, double addition is feasible, providing highly colored dyes displaying remarkable electrochemical properties.

© 2011 Elsevier Ltd. All rights reserved.

The term 'push–pull' has been used to describe conjugated compounds that have an electron donor group (D) and an electron withdrawing (A) group that exhibit intramolecular charge transfer (ICT) through the π-conjugated bridge (also called a D–π–A system). ICT character derives from the molecular push–pull structure and has been largely investigated for optical–electrical applications, such as in light-emitting devices,[1,2] optical imaging of living tissues,[3,4] nonlinear optical devices (NLO),[5,6] and solar cell materials.[7–10] It has been demonstrated that the combination of electron donor and electron withdrawing groups can efficiently modify the electronic signatures and chemical properties of the conjugated chromophore[7,11–13] such as seen in its optical absorption and electronic states (HOMO/LUMO). Over the last decade, most interest in push–pull systems has been focused on understanding structure–property relationships and the engineering of molecular materials with strong NLO responses.

BODIPY dyes are well known for their strong absorption, high solubility in common organic solvents, high fluorescence quantum yield, and their good chemical and photochemical stability.[14] Already known as laser dyes,[14] BODIPY derivatives are promising candidates for NLO applications. To date, however, only a few functionalised BODIPY based chromophores have been described for use in the field of two photon absorption for cell imaging or telecommunications[12–19] and overall the study of BODIPY based push–pull systems is rather limited.[7,11] The construction of a push–pull system based on the BODIPY scaffold should provide materials with new optical and electronic properties and thus might offer new opportunities for advanced optoelectronic devices.[9,20]

Here, we present a series of BODIPY bridged push–pull chromophores in which an electron donor group and an electron withdrawing group have been successively conjugated to the BODIPY core at the 2 and 6 positions. The optical and electrochemical properties have been investigated in detail. The introduction of anisole or benzaldehyde groups onto the BODIPY **1** at the 2,6 positions was performed by two successive Sonogashira coupling reactions under standard conditions (Scheme 1).[21] The ethynyl groups were selected not only as a means to attach the D/A groups to the chromophore, but also to extend the conjugation between the donor and the acceptor.[6] The dicyanomethylene group intended to function as an electron withdrawing entity was generated by a Knoevenagel condensation[22] on the aldehyde **3** with malononitrile in dichloromethane at reflux, leading to the purple compound **4** (Scheme 1). Some difficulties in the purification and identification of compound **4** were encountered due to its poor solubility in common solvents. Intermolecular aromatic π–π stacking and anti-parallel dipole–dipole interactions in solution favor molecular aggregation. This is a common practical problem that has been widely discussed in regard to push–pull chromophore synthesis.[23–25] The strategy often applied is to introduce bulky substituents onto the push–pull chromophore scaffold in order to increase the steric hindrance and prevent aggregation, therefore providing better solubility.[23,25] We have previously shown that introduction of diethynyl-groups on

* Corresponding authors. Tel.: +33 3 68 85 26 89; fax: +33 3 68 85 27 61 (R.Z.).
E-mail addresses: ziessel@unistra.fr, ziessel@chimie.u-strasbg.fr (R. Ziessel).

0040-4039/$ - see front matter © 2011 Elsevier Ltd. All rights reserved.
doi:10.1016/j.tetlet.2011.07.028

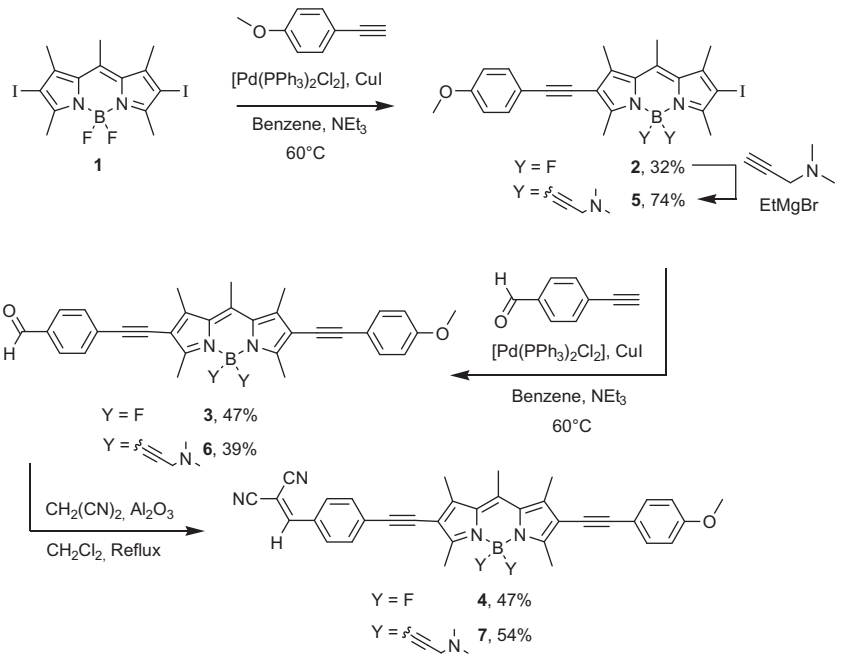

Scheme 1. Synthesis of BODIPY derivatives **2**–**7**.

the boron atom of the BODIPY core by using the appropriate Grignard reagents can indeed efficiently prevent the formation of aggregates and increase the solubility.[26,27] After the replacement of the fluorides of dye **2** using the Grignard reagent of dimethylaminopropyne to give **5**, the same procedure as used to obtain **4** gave the dicyanomethylene derivative **7** (Scheme 1). Compound **9** was synthesized similarly in order to compare its optical properties with those of compounds **4** and **7** (Scheme 2). Dye **9** is less conjugated than **4** and therefore has a better solubility in common organic solvents.

In order to improve the dipole moment strength along the BODIPY molecular axis, more powerful electron donor and electron withdrawing groups are required. This must, however, be associated with good solubility of the new dyes and a means of achieving this desirable combination was suggested by the recent work of Diederich and co-workers on the reaction of tetracyanoethene (TCNE) with electron rich alkyne derivatives.[28–31] The donor-substituted alkyne groups undergo a [2+2] cycloaddition reaction with TCNE, followed by the formation of an intermediate cyclobutene which subsequently undergoes ring opening leading to the 1,1,4,4-tetracyanobuta-1,3-diene (TCBD) derivatives (Scheme 3).

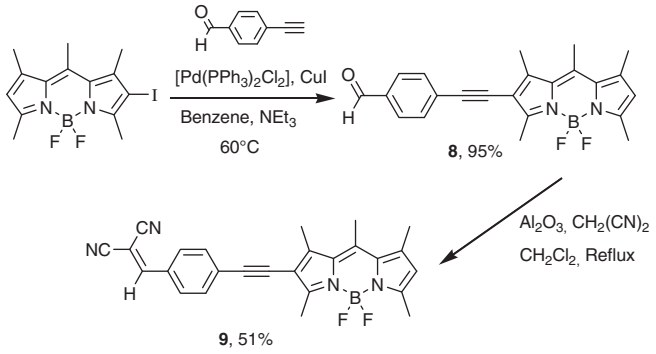

Scheme 2. Synthesis of BODIPY derivative **9**

The TCBD unit exhibits a strong acceptor character and imports a good solubility in common solvents due to the non-planarity of the molecule which efficiently prevents the formation of aggregates.[28,32]

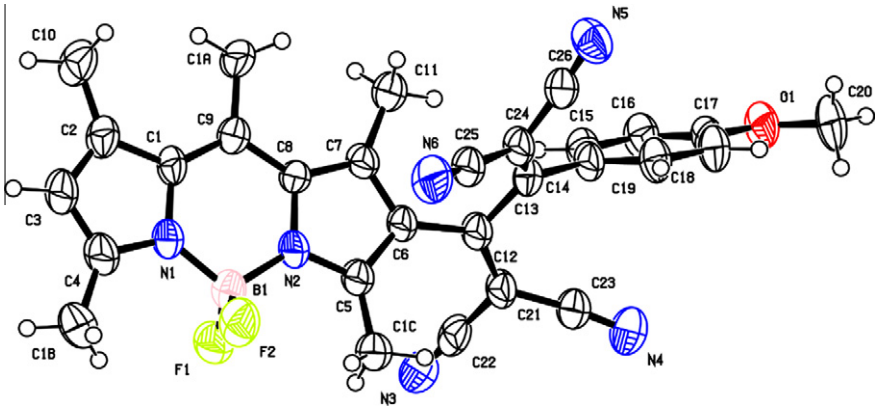

Scheme 3. ORTEP view of dye **11**. Displacement ellipsoids are drawn at 30% probability level.

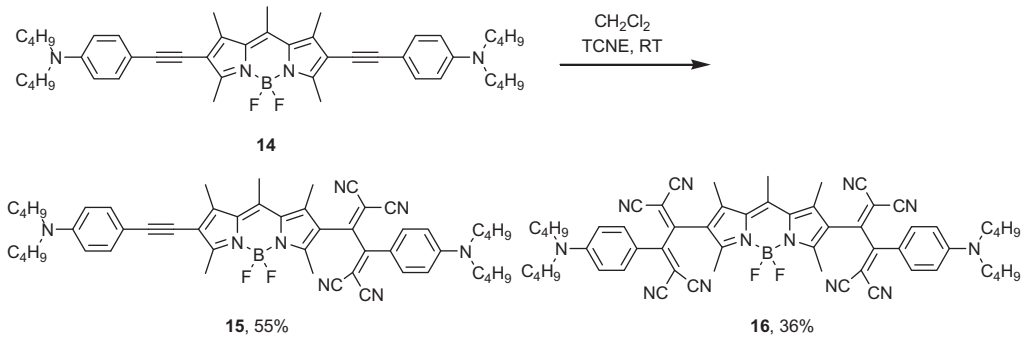

Scheme 4. Synthesis of dyes **15** and **16**.

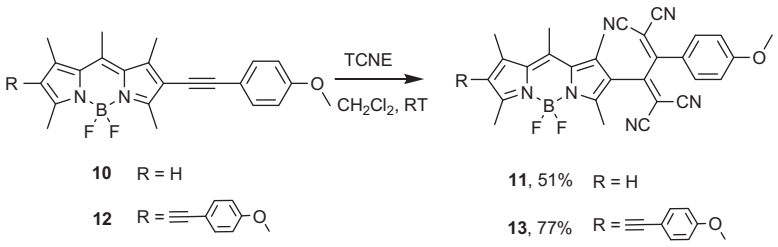

Figure 1. Synthesis of BODIPY derivatives **11** and **13**.

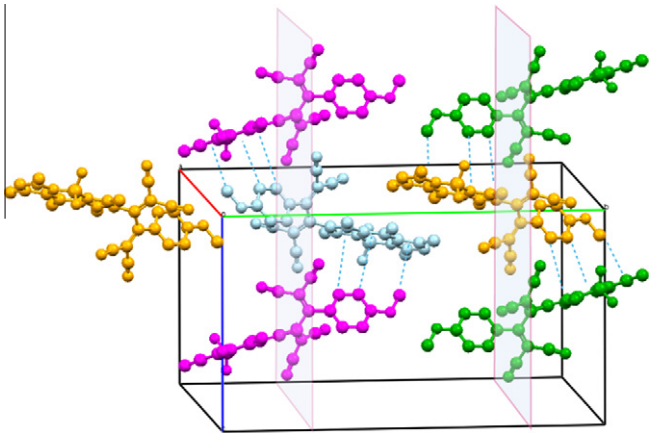

Figure 2. Packing view of dye **11** in cyan at general position *x*, *y*, *z*. In gold, molecules related by a center of inversion, in magenta, by c-glide planes (in transparency) and in green by a two-fold screw axis. Dashed lines indicate non-conventional hydrogen bonds.

The BODIPYs **10** and **12** containing ethynyl donor groups at the 2,6 positions were selected to react with TCNE in dichloromethane at room temperature, leading to the substituted TCBDs **11** and **13** in good yields (Fig. 3). Interestingly, the reaction of dye **12** with TCNE in a proportion of 1:2.2 gives the mono substituted derivative **13** in 77% yield. Despite the use of an excess of TCNE, the mono-insertion was principally observed, whereas no selectivity was observed during reaction of dye **14** with TCNE (Scheme 4). Compound **14** was synthesized according to the literature[21] then reacted with TCNE in a proportion of 1:1.3 under the standard reaction conditions. This gave the mono and di-substituted derivatives **15** and **16** in 55% and 36% isolated yields, respectively. The TCNE was totally consumed in the reaction, indicating that the dibutylamino moiety of **14** reacts more readily with TCNE than the anisole unit of **12**.

The molecular structure of compound **11** was determined by X-ray diffraction on a single crystal. The BODIPY core remains planar. The two dicyanovinyl (DCV) residues project in opposite directions, with an interplanar dihedral angle (C24–C13–C12–C21) of 38.2° (Fig. 1). The DCV moiety adjacent to the BODIPY twists out of the BODIPY plane with a torsion angle (C5–C6–C12–C21) of 43.7°, while the other DCV moiety twists in the opposite sense, with a torsion angle (C7–C6–C12–C13) of 43.5°. The torsion angle between the anisole ring and the adjacent DCV (C24–C13–C14–C19) is 47.1° and that with the other DCV (C12–C13–C14–C15) is 46.7°. Due to the strongly electron withdrawing TCBD groups, the C7–C6 bond (1.41 Å) is significantly longer than the C2–C3 bond (1.36 Å).

Molecules of compound **11** are all aligned in the crystalline state along the longest dimension of the unit cell, that is, the ***b*** axis, but without developing efficient π–π stacking interactions, whereas TCBD moieties are segregated into layers along the glide planes at positions $y = \frac{1}{4}$ and $\frac{3}{4}$ (Fig. 2). Among the numerous weak interactions which mediate the crystal packing of these molecules, for example, CH_3(methoxy-)···O(methoxy at $-x, -y, -z$), C–H···F making molecular chains along the [1 0 0] direction, C–H(methoxybenzyl group···π (BODIPY) hydrogen bonds between molecules related by the ***c*** glide planes, three out of the four TCBD nitrogen accept C_{sp2} or 3-H bonds from close neighbors with distances ranging between 2.4 and 2.7 Å.

The optical properties of the push–pull chromophores were evaluated in different solvents. Table 1 contains selected data for species other than the TCBD derivatives (see ahead). In solution, all these compounds show a strong S_0–S_1 transition between $\lambda \approx 540$–570 nm with an absorption coefficient in the 60,000–90,000 M^{-1} cm^{-1} range, unambiguously assigned to the boradiazaindacene chromophore.[33] In EtOH, a decrease of the extinction coefficient for both formyl derivatives **3** and **6** were observed. This fact may be attributed to the poor solubility of the compounds in EtOH. At higher energy, two weak broad bands centered around 410 nm and 350 nm, can be attributed to a charge transfer absorption[33] and the S_0–S_2 transition of the BODIPY moiety, respectively.[34] π–π* transitions with vibronic structure are observed at 230–320 nm for the phenyl groups. In CH_2Cl_2, the BODIPY dyes show emission maximum in the 561–611 nm range. The

Table 1
Optical properties of selected BODIPY derivatives

Compounds	λ_{abs} (nm)	ε (M^{-1} cm^{-1})	λ_{em} (nm)	Φ[a] (%)	τ (ns)	k_r[b]	k_{nr}[b]
2 (CH_2Cl_2)	543	57,000	606	6	0.7	8.6	134.3
3 (Dioxan)	561	80,000	604	42	2.6	16.2	22.3
3 (CH_2Cl_2)	563	36,000	611	28	1.7	16.5	42.4
3 (EtOH)	556	12,000	614	16	0.9	17.8	93.3
4 (Dioxan)	565	73,000	610	46	2.4	19.2	22.5
4 (CH_2Cl_2)	569	82,000	616	28	1.7	16.5	42.4
4 (EtOH)	563	74,000	612	16	1.1	14.5	76.4
5 (CH_2Cl_2)	539	52,000	600	3	1.4	2.1	69.3
6 (Dioxan)	555	57,000	591	76	3.2	23.8	7.5
6 (CH_2Cl_2)	559	65,000	603	36	2.7	13.3	23.7
6 (EtOH)	555	36,000	598	41	2.5	16.4	23.6
7 (Dioxan)	562	75,000	597	73	3.1	23.5	8.7
7 (CH_2Cl_2)	567	85,000	606	32	1.5	21.3	45.3
7 (EtOH)	562	75,000	600	15	1.1	13.6	77.3
9 (CH_2Cl_2)	535	94,000	561	53	2.3	23.0	20.4
10(CH_2Cl_2)	526	55,100	591	17	1.7	10.0	48.8

[a] Quantum yield determined in dilute solution (1×10^{-6} M) using rhodamine 6G as reference ($\varphi_F = 0.78$ in water, $\lambda_{exc} = 488$ nm).[38]
[b] All φ_F are corrected for changes in refractive index. k_r (10^7 s^{-1}) and k_{nr} (10^7 s^{-1}) were calculated using the following equations: $k_r = \varphi_F/\tau$, $k_{nr} = (1 - \varphi_F)/\tau$.

fluorescence quantum yields are in the 28–53% range, with the exception of the intermediate iodo-substituted compounds **2** and **5**, for which the fluorescence is dramatically reduced due to a faster nonradiative decay, suggesting a fast intersystem crossing from the singlet excited state to the triplet state.[21]

The absorption spectra of the dicyanomethylene derivatives **4**, **7** and **9** in dichloromethane show intense absorption around 480–630 nm with molar absorption coefficients in the 75,000–94,000 M^{-1} cm^{-1} range (Fig. 3). In the absence of the anisole group, compound **9** shows hypsochromic shifts relative to compound **4** of 34 and 55 nm in absorption and emission, respectively. In addition, **9** has a relatively small Stokes shift (866 cm^{-1}) with a higher quantum yield (53%) and longer decay time (2.3 ns). The absorption band centered at 420 nm with absorption coefficients in the 15,000–20,000 M^{-1} cm^{-1} range can be attributed to a charge transfer absorption band. The absorption centered on 350 nm can be attributed to the S_0–S_2 transition with absorption coefficients in the range of 15,000–18,000 M^{-1} cm^{-1}. This transition is also more intense than in common BODIPYs.[33] Surprisingly, no significant solvatochromism is observed for any of the push–pull dyes, with variation of less than 6 nm from solvents with weak dipole moments to solvents with a stronger dipole.

The influence of the solvent is more important on the fluorescence with a strong decrease of the quantum yields (Φ) and the lifetime (τ) when the dipole moment of the solvent increases. Conversely, the Stokes shifts increase slightly in more polar solvents. For **7**, the quantum yield (φ) and lifetime (τ) decrease when the solvent changes from dioxane (0.73, 3.1 ns) to EtOH (0.15, 1.1 ns). The rate of non-radiative decay k_{nr} increases (about nine times) while that of radiative decay k_n remains similar. The small changes in Stokes shift in solvents with various dipole moments may indicate that the difference in dipole moments between the excited state and the ground state is small.[33,35]

The TCBD BODIPY dyes **13**, **15** and **16** show high solubility in common solvents. The UV/Vis absorption spectra of all three molecules display a similar broad, less band between 450 and 700 nm, with molar absorption coefficients in the 35,000–80,000 M^{-1} cm^{-1} range (Fig. 4). In comparison with the parent BODIPY **12**, the lowest energy absorption maximum of **13** shows a bathochromic shift of 25 nm. For **15** and **16**, the formation of mono- and di-TCBD moieties leads to bathochromic shifts of 25 and 40 nm, respectively, compared with **14**. The broad absorption band may be due to an inhomogeneous distribution of the solvation sphere. Interestingly, for **15** at shorter wavelengths, two overlapping absorption bands are observed between 260 and 400 nm, corresponding to CT

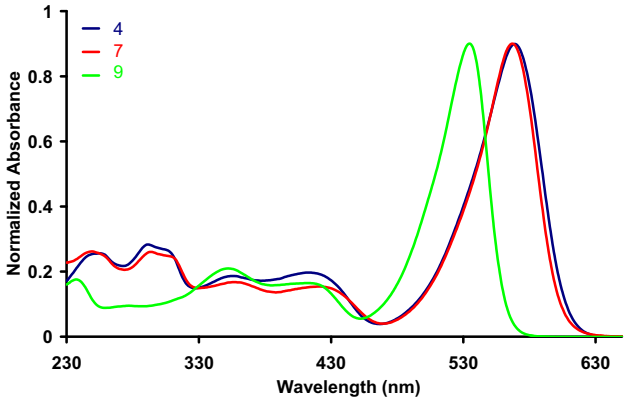

Figure 3. Normalized absorption spectra of **4** (dark blue), **7** (red) and **9** (green) in CH_2Cl_2.

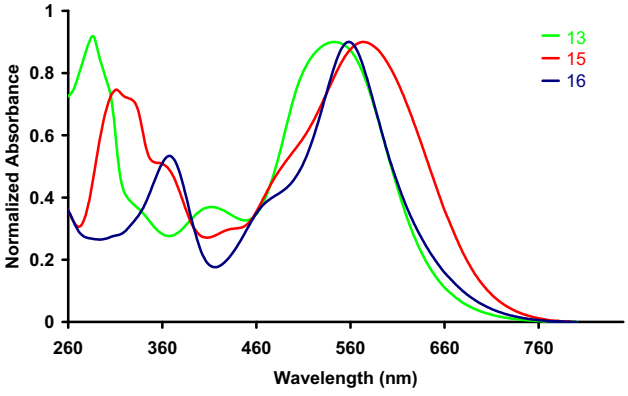

Figure 4. Normalized absorption spectra of **13** (green), **15** (red), and **16** (dark blue) in dioxane.

between the amino group and the adjacent TCBD, and to the π–π^* transition of the free alkylaminophenylethylene group, the latter being absent in the case of **16**. The fluorescence of the TCBD dyes **13**, **15**, and **16** is completely quenched.

The electrochemical properties of selected dyes were evaluated by cyclic voltammetry (Table 2). Compound **12** was used as reference to compare with dyes **4** and **13**. For dyes **4** and **12**, both are

Table 2
Electrochemical data of selected BODIPYs[a]

Compounds	E°_{ox} [V] (ΔE [mV])	E°_{red} [V] (ΔE [mV])
4	+1.09 (irrev)	−1.05 (irrev), −1.12 (90)
12	+1.01 (irrev)	−1.10 (96)
13	+1.27 (irrev)	−0.25 (64), −0.73 (69), −1.48 (78)
14	+0.65 (irrev), +0.75 (irrev), +1.15 (76)	−1.16 (106)
15	+0.76 (irrev), +1.26 (71)	−0.41 (83), −0.80 (144), −1.57 (irrev)
16	+1.27 (80)	−0.29 (76), −0.42 (85), −0.81 (120), −0.95 (164)

[a] Cyclic voltammetry carried out in deoxygenated CH_2Cl_2 solutions, containing 0.1 M $TBAPF_6$, at a solute concentration range of 1.5×10^{-3} M, at 20 °C. Potentials were standardized using added ferrocene (Fc) as internal reference and converted to SCE assuming that $E_{1/2}$ (Fc/Fc^+) = +0.38 V (ΔE_p = 70 mV) versus SCE. Error in half-wave potentials is ±15 mV. When the redox process is irreversible the peak potential (E_{ap} or E_{cp}) is quoted.

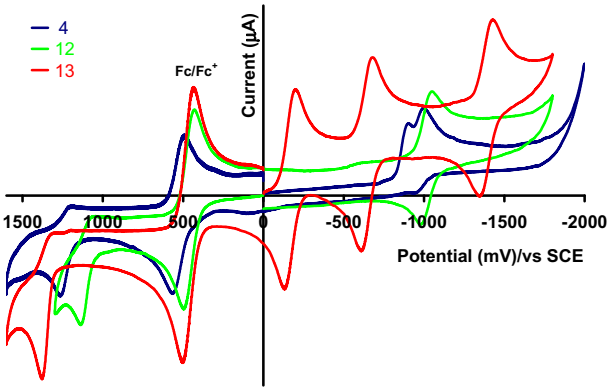

Figure 5. Cyclic voltammetry of **4** + ferrocene (dark blue), **12** + ferrocene (green), and **13** + ferrocene (red).

characterized by an irreversible oxidation wave at +1.09 and +1.01 V, respectively, corresponding to the one-electron oxidation of the BODIPY moiety to the radical cation (Fig. 5). On the reduction scans, a single reversible peak is observed at −1.10 V for dye **12** and −1.12 V for **4** and can be unambiguously attributed to the formation of the π-radical anion of the BODIPY core.[11,29,36] For **4**, an additional irreversible reduction of the dicyanovinyl group was observed at −1.05 V, this being in the expected potential range for a dicyanovinyl residue.[37]

For dye **13**, on the oxidation scans, an irreversible wave was observed at +1.27 V and can be attributed to the BODIPY moiety undergoing one-electron oxidation. Compared with dye **12**, it is clear that the TCBD residue makes the BODIPY moiety more difficult to oxidize by 250 mV. On the reduction scans, interestingly, three reversible peaks are observed at −0.25, −0.73, and −1.48 V, corresponding to the successive one-electron reductions of the dicyanovinyl (DCV) groups and the BODIPY moiety, respectively. Due to the electrostatic effect, the second reduction of the DCV moiety is made more difficult by 480 mV and the reduction of the BODIPY moiety is more difficult by 380 mV.

The electrochemical properties of dye **14** are shown in Fig. 6. Three oxidation waves are observed at +0.65, +0.75 and +1.15 V. The first two close but resolvable irreversible one-electron oxidation waves can be attributed to the successive oxidation of the two dibutylamino moieties, indicating an effective electronic interaction between both groups through the π-conjugated BODIPY core. The third oxidation wave can be attributed to the formation of the BODIPY radical cation. The reversible reduction peak observed at −1.16 V corresponds to the formation of the BODIPY radical anion.

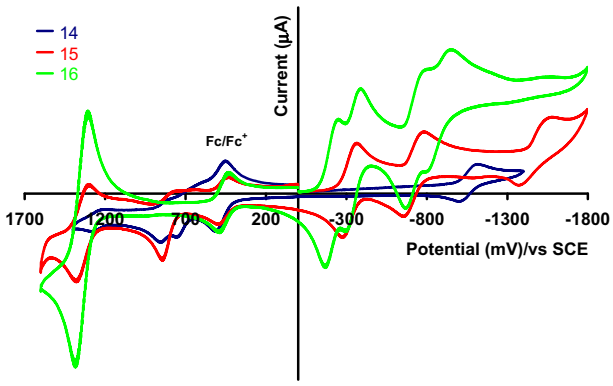

Figure 6. Cyclic voltammetry of TCBDs dyes **14** + ferrocene (dark blue), **15** + ferrocene (red), and **16** + ferrocene (green).

For dye **15**, the first irreversible wave at +0.76 V can be unambiguously assigned to the one-electron oxidation of the free amino group at the opposite side of the TCBDs residue (Fig. 6). The TCBD group clearly renders the oxidation of the adjacent amino group more difficult due to a pronounced electron withdrawing effect. The second reversible but not well resolved oxidation wave at +1.26 V is more difficult to assign. In comparison with **14**, the peak can be attributed either to the amino group adjacent to the TCBD, or to the BODIPY oxidation to form the radical cation. For **13**, two well resolved reversible reduction steps at −0.41, −0.80 V, and a third quasi-reversible reduction step at −1.57 V can be attributed to the successive one-electron reductions of the dicyanovinyl (DCV) groups and the BODIPY moiety, respectively. The reduction of BODIPY core is made more difficult by the TCBD residue by 410 mV.

More interestingly, for dye **16** a single reversible oxidation peak is observed at +1.27 V. The fact that the current integration of this peak is double that for the first reduction peak at −0.29 V, indicates that both amino groups oxidize at the same potential due to the sterically enforced deconjugation induced by the TCBD residues. Furthermore, in comparison with **15**, the oxidation of the BODIPY core will be shifted to a higher potential due to the presence of two TCBDs residues. It is likely that the potential falls outside the accessible electrochemical window (+1.6 V vs SCE). The remarkable three reversible and fourth quasi-reversible reductions steps observed at −0.29, −0.42, −0.81, and −0.95 V, respectively, correspond to the successive one electron reductions of the four DCV moieties. The reduction of the BODIPY core is obviously made more difficult by the double TCBD residues, and is probably outside the accessible electrochemical window (−1.6 V vs SCE).

In summary, a series of BODIPY based push–pull chromophores have been prepared and their optical and electrochemical properties have been investigated. Interesting electrochemical properties of the TCBD BODIPY dyes were observed due to the strong electron withdrawing groups. There appears to be an effective electronic conjugation along the 2,6-molecular axis. Further investigations of the nonlinear optical properties of these push–pull dyes are currently in process.

Acknowledgments

We acknowledge the CNRS for providing research facilities and financial support and Professor Jack Harrowfield (ISIS in Strasbourg) for commenting on the manuscript before publication.

References and notes

1. Zhou, Y.; Xiao, Y.; Chi, S.; Qian, X. *Org. Lett.* **2008**, *10*, 633–636.

2. Dong, Y.; Bolduc, A. a.; McGregor, N.; Skene, W. G. *Org. Lett.* **2011**, *13*, 1844–1847.
3. Barsu, C.; Cheaib, R.; Chambert, S.; Queneau, Y.; Maury, O.; Cottet, D.; Wege, H.; Douady, J.; Bretonniere, Y.; Andraud, C. *Org. Biomol. Chem.* **2010**, *8*, 142–150.
4. Lord, S. J.; Conley, N. R.; Lee, H.-l. D.; Samuel, R.; Liu, N.; Twieg, R. J.; Moerner, W. E. *J. Am. Chem. Soc.* **2008**, *130*, 9204–9205.
5. Marder, S. R.; Kippelen, B.; Jen, A. K. Y.; Peyghammbarian, N. *Nature (London)* **1997**, *388*, 845–851.
6. LeCours, S. M.; Guan, H.-W.; DiMagno, S. G.; Wang, C. H.; Therien, M. J. *J. Am. Chem. Soc.* **1996**, *118*, 1497–1503.
7. Collado, D.; Casado, J.; González, S. R.; Navarrete, J. T. L.; Suau, R.; Perez-Inestrosa, E.; Pappenfus, T. M.; Raposo, M. M. M. *Chem. Eur. J.* **2011**, *17*, 498–507.
8. Burckstummer, H.; Kronenberg, N. M.; Meerholz, K.; Würthner, F. *Org. Lett.* **2010**, *12*, 3666–3669.
9. Erten-Ela, S.; Yilmaz, M. D.; Icli, B.; Dede, Y.; Icli, S.; Akkaya, E. U. *Org. Lett.* **2008**, *10*, 3299–3302.
10. Chu, T.-Y.; Lu, J.; Beaupré, S. .; Zhang, Y.; Pouliot, J.-R. m.; Wakim, S.; Zhou, J.; Leclerc, M.; Li, Z.; Ding, J.; Tao, Y. *J. Am. Chem. Soc.* **2011**, *133*, 4250–4253.
11. Ziessel, R.; Retailleau, P.; Elliott, K. J.; Harriman, A. *Chem. Eur. J.* **2009**, *15*, 10369–10374.
12. Zhou, E.; Tan, Z. a.; Yang, Y.; Huo, L.; Zou, Y.; Yang, C.; Li, Y. *Macromolecules* **2007**, *40*, 1831–1837.
13. Wakatsuki, Y.; Yamazaki, H.; Kobayashi, T.; Sugawara, Y. *Organometallics* **1987**, *6*, 1191–1196.
14. (a) Loudet, A.; Burgess, K. *Chem. Rev.* **2007**, *107*, 4891–4932; (b) Ulrich, G.; Ziessel, R.; Harriman, A. *Angew. Chem., Int. Ed.* **2008**, *47*, 1184–1201.
15. Bouit, P. A.; Kamada, K.; Feneyrou, P.; Berginc, G.; Toupet, L.; Maury, O.; Andraud, C. *Adv. Mater.* **2009**, *21*, 1151–1154.
16. Didier, P.; Ulrich, G.; Mely, Y.; Ziessel, R. *Org. Biomol. Chem.* **2009**, *7*, 3639–3642.
17. Zheng, Q.; Xu, G.; Prasad, P. *Chem. Eur. J.* **2008**, *14*, 5812–5819.
18. Zhang, D.; Wang, Y.; Xiao, Y.; Qian, S.; Qian, X. *Tetrahedron* **2009**, *65*, 8099–8103.
19. Zheng, Q.; He, G. S.; Prasad, P. N. *Chem. Phys. Lett.* **2009**, *475*, 250–255.
20. Kolemen, S.; Cakmak, Y.; Erten-Ela, S.; Altay, Y.; Brendel, J.; Thelakkat, M.; Akkaya, E. U. *Org. Lett.* **2010**, *12*, 3812–3815.
21. Bonardi, L.; Ulrich, G.; Ziessel, R. *Org. Lett.* **2008**, *10*, 2183–2186.
22. Knoevenagel, E. *Ber. Der. Deut. Chem. Gesell.* **1898**, *31*, 2596–2619.
23. Würthner, F.; Wortmann, R.; Meerholz, K. *ChemPhysChem* **2002**, *3*, 17–31.
24. Moore, A. J.; Chesney, A.; Bryce, M. R.; Batsanov, A. S.; Kelly, J. F.; Howard, J. A. K.; Perepichka, I. F.; Perepichka, D. F.; Meshulam, G.; Berkovic, G.; Kotler, Z.; Mazor, R.; Khodorkovsky, V. *Eur. J. Org. Chem.* **2001**, 2671–2687.
25. Würthner, F.; Yao, S. *Angew. Chem., Int. Ed.* **2000**, *112*, 2054–2057.
26. Goze, C.; Ulrich, G.; Ziessel, R. *J. Org. Chem.* **2007**, *72*, 313–322.
27. (a) Rousseau, T.; Cravino, A.; Bura, T.; Ulrich, G.; Ziessel, R.; Roncali, J. *Chem. Commun.* **2009**, 1673–1675; (b) Rousseau, T.; Cravino, A.; Bura, T.; Ulrich, G.; Ziessel, R.; Roncali, J. J. *J. Mater. Chem.* **2009**, *19*, 2298–2300; (c) Niu, S. L.; Massif, C.; Ulrich, G.; Ziessel, R.; Renard, P.-Y.; Romieu, A. *Org. Biomol. Chem.* **2010**, *9*, 66–69.
28. Kato, S.-I.; Diederich, F. *Chem. Commun.* **2010**, *46*, 1994–2006.
29. Kato, S. I.; Kivala, M.; Schweizer, W.; Boudon, C.; Gisselbrecht, J. P.; Diederich, F. *Chem. Eur. J.* **2009**, *15*, 8687–8691.
30. Jarowski, P. D.; Wu, Y.-L.; Boudon, C.; Gisselbrecht, J.-P.; Gross, M.; Schweizer, W. B.; Diederich, F. *Org. Biomol. Chem.* **2009**, *7*, 1312–1322.
31. Reutenauer, P.; Kivala, M.; Jarowski, P. D.; Boudon, C.; Gisselbrecht, J.-P.; Gross, M.; Diederich, F. *Chem. Commun.* **2007**, 4898–4900.
32. Esembeson, B.; Scimeca, M. L.; Michinobu, T.; Diederich, F.; Biaggio, I. *Adv. Mater.* **2008**, *20*, 4584–4587.
33. Qin, W.; Baruah, M.; Van der Auweraer, M.; De Schryver, F. C.; Boens, N. *J. Phys. Chem. A* **2005**, *109*, 7371–7384.
34. Karolin, J.; Johansson, L. B. A.; Strandberg, L.; Ny, T. *J. Am. Chem. Soc.* **1994**, *116*, 7801–7806.
35. (a) Demeter, A.; Berces, T.; Zachariasse, K. A. *J. Phys. Chem. A* **2001**, *105*, 4611–4621; (b) Druzhinin, S. I.; Kovalenko, S. A.; Senyushkina, T. A.; Demeter, A.; Januskevicius, R.; Mayer, P.; Stalke, D.; Machinek, R.; Zachariasse, K. A. *J. Phys. Chem. A* **2009**, *113*, 9304–9320.
36. Nepomnyashchii, A. B.; Cho, S.; Rossky, P. J.; Bard, A. J. *J. Am. Chem. Soc.* **2010**, *132*, 17550–17559.
37. Liu, Y.; Zhou, J.; Wan, X.; Chen, Y. *Tetrahedron* **2009**, *65*, 5209–5215.
38. Olmsted, J. *J. Phys. Chem.* **1979**, *83*, 2581–2584.